

Quantum confinement induced oscillatory electric field on a stepped Pb(111) film and its influence on surface reactivity

Xiaojie Liu,^{1,2} Cai-Zhuang Wang,^{2,*} Myron Hupalo,² Hai-Qing Lin,^{1,†} Kai-Ming Ho,² and Michael C. Tringides²

¹Beijing Computational Science Research Center, Beijing, 100084, People's Republic of China

²Ames Laboratory—U.S. Department of Energy, and Department of Physics and Astronomy, Iowa State University, Ames, Iowa, 50011, USA

(Received 5 December 2012; revised manuscript received 25 November 2013; published 6 January 2014)

When the thickness of ultrathin metal films approaches the nanometer scale comparable to the coherence length of the electrons, significant effects on the structure stability and the electronic properties of the metal films emerge due to electron confinement and quantization of the allowed electronic states in the direction perpendicular to the film. Using first-principles calculations, we showed that such quantum size effects can induce oscillatory electrostatic potential and thus alternating electric field on the surface of the wedge-shaped Pb(111) films. The alternating electric field has significant influence on surface reactivity, leading to selective even- or odd-layer adsorption preference depending on the charge state of the adatoms, consistent with the odd-layer preference of higher Mg coverage on wedge-shaped Pb(111) films, as observed in experiment.

DOI: [10.1103/PhysRevB.89.041401](https://doi.org/10.1103/PhysRevB.89.041401)

PACS number(s): 73.21.Fg, 68.43.Bc, 68.37.Ef, 73.61.At

Manipulating and controlling the surface chemical reactivity on metal thin films is an interesting topic in physics and chemistry, since metal surfaces play an important role in catalysis, molecular self-organization, and corrosion processes. Electrons in thin metal films are confined in the direction perpendicular to the film surface, resulting in discrete energy level associated with the so-called quantum well state (QWS) [1–3]. Such quantum size effects (QSEs) can be utilized to manipulate the electronic structures of the metal films as a function of film thickness, thus providing a mechanism for controlling the chemical reactivity on the surface. For example, a bilayer oscillatory behavior of the stability and properties (including the work function) of Pb(111) films due to the QSE have been reported by many experimental and theoretical studies [3–11]. Recent experiments also demonstrated that the QSE can cause selective adsorption and enhancement of chemical process on the terraces of wedge-shaped thin Pb(111) films formed on stepped Si(111) substrate [9–12]. Nevertheless, the microscopic mechanisms that relate the QSE to the experimentally observed selective chemical reaction are still not well understood, although some correlations between the surface reactivity and electronic properties (e.g., work function, density of states at Fermi level) have been discussed [9–12].

In this Rapid Communication, we investigate how QSE can control the selective adsorption and chemical processes on stepped or wedge-shaped Pb(111) films. Unlike all the previous theoretical studies which have focused on the properties of separate uniform height islands, we investigate the situation when several Pb thin strips with different thicknesses are brought into contact to form a stepped or wedge-shaped thin film. Using first-principles calculations, we show that QSE will induce a modulated oscillatory electrostatic potential on the surface of stepped or wedge-shaped Pb(111) films. This modulated electrostatic potential will cause an alternating electric field across the strips of different thickness on the wedge and influence the growth morphology and reactivity on

the flat top of the wedge-shaped Pb(111) films as observed experimentally. Such a QSE induced electric field modulation mechanism would be used to design metal film geometries for desirable controlling of nanostructure morphologies and selective chemical reactions. We note that although QSEs in metal films have been studied intensively for over a decade, such alternating electric field along the parallel direction on the surface of the wedge-shaped metal films has not been reported. The effects of such an electric field were not considered in all previous theoretical interpretations of the observed interesting phenomena on wedge-shaped Pb(111) films since these studies are based on calculation results of individual films with uniform height and the proximity of two domains of different heights was not taken into account.

The supercell used in our calculations is a Pb(111) thin slab with flat top and stepped bottom as shown in Fig. 1. In this supercell, the thin domain is 4 layers while the thick domain is 5 layers. The dimension of the super cell in the x - y plane is 20×1 and with periodic boundary conditions. The dimension along the z direction is 45.64 \AA which allows at least 34.2 \AA of vacuum region to separate the slab. It is worth mentioning that due to the bilayer oscillatory behavior of the energy and physical properties of the Pb(111) film as a function of the film thickness, the supercell as shown in Fig. 1 with periodic boundary conditions can also be used to model the wedge-shaped Pb(111) films employed in several recent experiments [4,5,9–12].

The first-principles calculations are performed based on the density functional theory (DFT) using the Vienna *ab initio* simulation package (VASP) [13,14], in which a plane wave basis set is used to solve Kohn-Sham equations. The generalized gradient approximation (GGA) of Perdew *et al.* [15], including dipole moment corrections [16], is employed in the calculations. Valence electrons are treated explicitly and their interactions with ionic cores are described by ultrasoft pseudopotentials [17]. For Pb atom, the $6s$, $6p$, and $5d$ electrons are treated as valence electrons. The wave functions are expanded in a plane wave basis set with an energy cutoff of 400 eV . A K -point grid of $1 \times 40 \times 1$ is used in the calculations.

*wangcz@ameslab.gov

†haiqing0@csrc.ac.cn

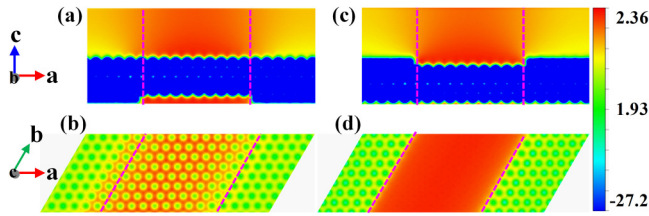


FIG. 1. (Color online) Electrostatic potential (units: eV) on the top (a) and (b) and bottom (c) and (d) surfaces of a stepped 5-4-5 layers Pb(111) film. The side views (a) and (c) show the potentials as recorded on the vertical cutting plane through the middle of the unit cell used in the calculation. The top views (b) and (d) show the potential on a horizontal cutting plane at 2.4 and 2.3 Å above the surface, respectively. The blue color indicates the potential from 0 to -27.2 eV. The directions of the lattice vectors a , b , and c are also given.

In Fig. 1, the electrostatic potential distributions on both surfaces of the stepped Pb(111) film obtained from the first-principles calculations are plotted. Oscillatory modulated electrostatic potentials on both sides of the stepped film are observed. The domain with thickness of 4 layers has higher electrostatic potential while the potential in the 5-layer domain is approximately 0.20 eV lower. The local potential difference between 4- and 5-layer domains can be attributed to the work function difference between the 4-layer and 5-layer thin films caused by QSE [1,2,5,7,11,12]. For metal film with lower work function (in this case, a 5-layer film has a lower work function than a 4-layer film), its Fermi level is higher since the work done to move an electron from its Fermi surface to the vacuum is smaller. Therefore, when the two metal films with different work functions are brought into contact, electrons from the domain with lower work function will flow to the domain with higher work function until the whole sample reaches the same Fermi level. In Fig. 2, the local charge distribution is calculated in the energy window from the Fermi level to 1.43 eV below. The electron redistribution is indeed seen from our calculations in Fig. 2 where the 4-layer region gains more electrons from the 5-layer region.

The consequence of the electron transfer induced by the work function difference is that the 4-layer region will be negatively charged and exhibit higher electrostatic potential for electrons and vice versa for the 5-layer region as shown in

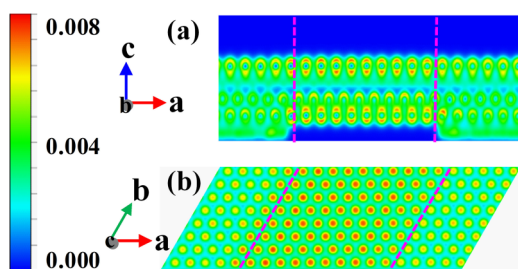


FIG. 2. (Color online) The density of charge as integrated over an energy window of 1.43 eV below the Fermi energy. (a) Charge distribution on the vertical plane cutting through the middle of the unit cell; (b) charge distribution on the horizontal plane cutting at 1.1 Å above the surface.

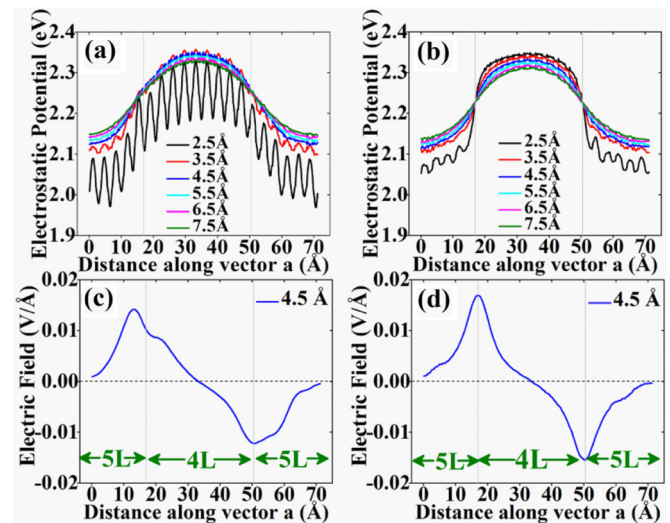


FIG. 3. (Color online) (a) and (b) The line scan of electrostatic potential along the lattice vector a direction from Figs. 1(b) and 1(d) at different heights from the Pb(111) top [Fig. 1(b)] and bottom [Fig. 1(d)] surface, respectively. (c) and (d) Electric field distribution induced by the QSE across the domain of different thickness calculated using the potential profile at the height of 4.5 Å: (c) for the flat-top surface and (d) for the stepped-bottom surface.

Fig. 1. More details about the potential profiles can also be seen from Figs. 3(a) and 3(b) where the line scans from Figs. 1(b) and 1(d) at different distances from the Pb(111) top and bottom surfaces, respectively, are plotted. On the plane parallel and close to the flat-top surface (e.g., approximately 2.5 Å from the nucleus of surface atom), the QSE induced a modulated potential with a valley-to-peak amplitude of ~ 0.20 eV on the top of the periodic atomic potential from the surface atoms. However, at a larger distance (e.g., about 4.5 Å above the surface), the atomic potential diminishes while the modulated potential persists. Similar modulated potential profiles are also seen from the bottom stepped surface on Fig. 3(b). We have also calculated the electrostatic potential profiles for two other lateral dimensions, i.e., 16×1 and 24×1 . The results from the 20×1 and 24×1 samples are very similar, indicating that our calculation using 20×1 is converged. We expect that as the lateral size gets larger, the electrostatic potential inside each domain will become flatter, but the electrostatic potential at the domain boundary region will be very similar regardless of the lateral size.

By taking the derivative of the electrostatic potentials along the line-scanned electrostatic potential profiles, we can evaluate the electric field distribution induced by the QSE across the domain of different thickness, as shown in Figs. 3(c) and 3(d), respectively. An alternating electric field across the domain of different thickness is observed with the largest field (more than 1.6×10^6 V/cm) at the domain boundary. The electric field decays rapidly away from the domain boundary and with the penetration length about 15 Å. In experimental samples where the domains are much wider (~ 100 Å), the electric field away from the domain boundary in the lateral direction should be very close to zero.

Wedge-shaped Pb(111) films grown on the stepped Si(111) surface exhibit a flat-top surface and a stepped-bottom surface

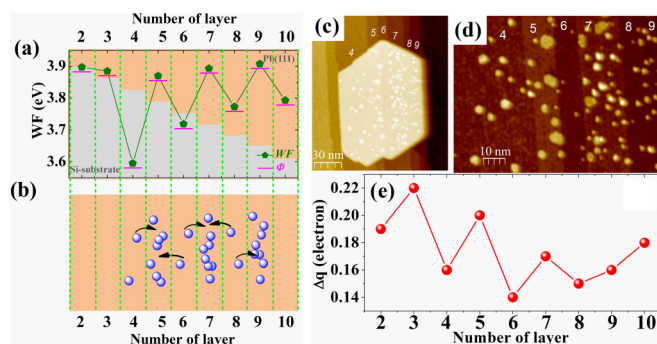


FIG. 4. (Color online) (a) A schematic drawing of the work function (green pentagon) and the related electrostatic potential Φ (pink line) on the flat-top surface of a wedge-shaped Pb(111) films. (b) Positively charged adsorbates distribution on different thickness of Pb(111) films driven by the alternating electric field across the wedge-shaped Pb(111) films. (c) and (d) STM images of the distribution of Mg islands density on the Pb(111) surface. (d) is enlarged from (c). The image in (c) is $150 \times 150 \text{ nm}^2$ while that in (d) is $86.1 \times 57.7 \text{ nm}^2$. Both (c) and (d) show the distribution of Mg island density on a stepped Pb substrate (quantum wedge) with terrace heights increasing from 4 to 9 layers as indicated. The STM image from (c) and (d) showing that both the island density and Mg coverage are higher on stable (5, 7, 9) than on the unstable heights (4, 6, 8). (e) Electron transfer (red solid circles) for Mg adatom on a Pb(111) film as the function of the film thickness. Note that because the height in experiment is measured from the wetting layer, the height labeled by most experiments is 1 layer less than the thickness of the films measured from the Si substrate layer. Therefore, the theoretical results shown in the figure have been shifted by 1 layer in order to match the heights labeled by experiment.

with a layer-by-layer change in film thickness across the wedge. Due to the bilayer oscillatory characteristics, such a Pb wedge film provides a unique geometric setup for studying surface adsorption and chemical reactivity controlled by QSE [9–11]. According to the first-principles calculations discussed above, the QSE should induce an oscillatory electrostatic potential on the flat top of the wedge-shaped Pb(111) films. As shown schematically in Fig. 4(a), the Pb(111) film with lower work function (WF) has relatively smaller local potential (Φ) for electrons. The even-odd oscillation of electrostatic potential on the wedge-shaped Pb(111) film will cause alternating electric field across the boundaries of the domains on the wedge. This alternating electric field would provide extra driving forces for the motion of adatoms or molecules on wedge-shaped Pb(111) films if the adatoms are charged. As schematically shown in Fig. 4(b), those particles with positive charge (e.g., due to charge transfer to the Pb films) will prefer to move to the region with larger work function, and thus larger electrostatic potential (for electrons), while those with negative ionic states will favor the lower potential region. The induced electric field at the domain boundary will drive the charged particles from the nonpreferred domain to the energetically favorable regions. Note that because the height in experiment is measured from the wetting layer, the height labeled by most experiments is 1 layer less than the thickness of the films from the Si substrate layer. Therefore, the theoretical

results shown in Fig. 4 have been shifted by 1 layer in order to match the heights labeled by experiment.

To validate the alternating electric field (or oscillatory electrostatic potential) mechanism on the adsorption behavior discussed above, we performed an experiment to study the behavior of Mg on wedge-shaped Pb(111) films. Large Pb islands were first grown at 240 K after depositing 1.5 monolayers (ML) at a low flux rate 0.1 ML/min. After the wetting layer is completed the Pb islands nucleate rapidly. The Pb island shown in Fig. 4(c) is a wedge island (mesa) that has nucleated over a region with bunched steps with dimensions $150 \times 150 \text{ nm}^2$. Because the step heights of Si(111) and Pb(111) differ only by 0.016 nm, the top of the Pb mesa is practically flat while the height increases by 1 layer on the adjacent low layer. The Pb island heights indicated by the number on the Fig. 4(c) and 4(d) include several “stable” and “unstable” heights. Such controlled wedge films have been the “laboratory” to study the role of QSE on several island properties and the use of lower temperature 240 K vs room temperature has guaranteed the layer height on the wedge-shaped Pb(111) films does not exceed 9 layers so the role of QSE is maximized.

After the surface is cooled to 89 K, 0.15 ML of Mg is deposited at a rate of 0.1 ML/min and the nucleation outcome is seen in Figs. 4(c) and 4(d) with Mg island density clearly modulated as a function of height. Both the Mg coverage and island density are higher on stable (odd-layer) than unstable (even-layer) Pb islands. Since the flux is uniform over the whole wedge-shaped Pb(111) island, Mg must have been transferred from unstable to stable heights on the Pb mesa. Because the electronegativity of Mg is much smaller than that of Pb (1.31 vs 2.33 in the Pauling scale), it is expected that Mg on Pb surface will transfer electrons to the Pb substrate. We have analyzed the charge transfer between the Mg adatom and Pb(111) films using first-principles calculations and quasi-atomic minimal basis orbitals (QUAMBOs) analysis [18–20]. We found that there is 0.15–0.22 electron transfer from Mg adatom to Pb(111) substrate depending on the thickness of the films as shown in Fig. 4(e). Based on the first-principles calculation results of electrostatic potential and electric field distributions shown in Fig. 3, the energy bias for a $\text{Mg}^{0.2+}$ to move across the even-odd domain boundary due to the QSE induced electric field would be about 40 meV. This energy bias due to electric field will cause the hopping barrier to be asymmetric and the adatom diffusion along and against the electric field direction will be different by a factor of ~ 200 at the experimental temperature of 89 K ($89 \text{ K} = 7.67 \text{ meV}$, $e^{40/7.67} = 185$). The cationic $\text{Mg}^{\delta+}$ on the wedge-shaped Pb(111) films should be influenced strongly by the alternating electric field and prefer the movement towards the odd layer where the electrostatic potential is higher. The experimental results clearly support the theoretical prediction. As seen in Figs. 4(c) and 4(d), the Pb film thickness ranges from 4 to 9 layers; both the island density and coverage of the Mg islands on the odd layers (5, 7, 9 layers) are generally larger than those of even layers.

The variation of terrace diffusion barrier with domain height for adatom on Pb(111) should also have important effects on the observed island density distribution. The effects of the electric field are additive to the diffusion barrier

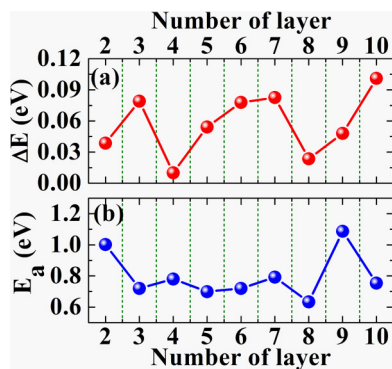


FIG. 5. (Color online) (a) Diffusion barrier (ΔE) and (b) adsorption energy (E_a) of Mg adatom on Pb(111) films as a function of film thickness which also has been shifted by one layer in order to match the heights labeled by experiment.

effects. Variation of island density has been observed in Mg deposition experiments in separate Pb(111) islands, with 7-layer islands the ones with the highest island density. Terrace diffusion barrier variation as a function of height from these experiments corresponds to at least 30 meV. Because the electric field is localized at the domain boundary (it is nonzero over approximately ten lattice constants) we expect its effects to be significant for narrow domains such as the wedge-shaped terrace used in the experiments. The island density on the separate islands should be determined only by the diffusion barrier. In order to get a more complete picture, we have also calculated the diffusion barrier as a function of film thickness for Mg adatom on Pb(111). The results are shown in Fig. 5(a). The diffusion barriers do not show odd-even oscillation and are not correlated with the observed odd-even oscillation in the Mg adsorbed island density observed in the experiment. The origin of this result is still not clear. In general, the diffusion barrier is expected to be correlated with the adsorption energy because larger adsorption energy will make the adatom more difficult to diffuse. We have also calculated the adsorption energy for Mg on Pb(111) as the function of film thickness as shown in Fig. 5(b). We found that the behavior of the diffusion barrier can be partially explained by the adsorption energy. Specifically, for Mg on 5–9 layers of Pb(111) film, we do observe the correlation between diffusion barrier and adsorption energy. However, such correlation between diffusion barrier and adsorption energy does not hold for every thickness Pb film. The origin

of this deviation deserves further investigations. On the other hand, the odd-even oscillating electric field discovered from the present calculation does correlate well with the odd-even adsorption preference of Mg on wedge-shaped Pb(111) films observed by experiment, which confirms the importance of the electric field for the island density modulation with wedge height.

In summary, we show that by the controlled growth of the wedge-shaped metal films and by the presence of different quantum-well states or different work functions at areas on its top, diffusion, adsorption, and self-assembly of atoms and molecules on metal thin film surface can be controlled. Using first-principles calculations, we showed that the quantum size effects can induce oscillatory electrostatic potential and thus alternating electric field on the flat top of wedge-shaped Pb(111) films. The preference of adsorption on even vs odd layers and assembly of adatoms or molecules on the top of the wedge-shaped Pb(111) films is therefore dependent on the charge state of the adsorbed atoms or molecules. Electron transfer will occur if the electronegativity of the adatom is different from the substrate. The QSE induced alternating electric field mechanism is consistent with our experiment observation for Mg nucleation on wedge-shaped Pb(111) films. We note that the island size and island density distribution on the wedge-shaped Pb(111) should also be governed by the variation of the Mg diffusion barrier with height and the additional biased diffusion across the domain at the top of the wedge. The combined role of unbiased diffusion (that is expected from QSE both on separate islands and the wedge-shaped films) and the role of the biased random walk due to the nonzero electric field across the domain boundary are also of interest, but are not explicitly addressed in this Rapid Communication. We believe the induced alternating electric field across the domain boundary would have great influence on the energy landscape of the diffusing charged adatoms and thus on the nucleation and growth morphology on the wedge-shaped Pb(111) films as compared to those on uniform thickness Pb(111) separate nanoislands. Further study along this line would be interesting.

Work at Ames Laboratory was supported by the U.S. Department of Energy, Basic Energy Sciences, Division of Materials Science and Engineering, including a grant of computer time at the National Energy Research Scientific Computing Center (NERSC) in Berkeley, CA under Contract No. DE-AC02-07CH11358.

- [1] F. K. Schulte, *Surf. Sci.* **55**, 427 (1976).
- [2] P. J. Feibelman, *Phys. Rev. B* **27**, 1991 (1983).
- [3] Z. Y. Zhang, Q. Niu, and C. K. Shih, *Phys. Rev. Lett.* **80**, 5381 (1998).
- [4] M. Hupalo, V. Yeh, L. Berbil-Bautista, S. Kremmer, E. Abram, and M. C. Tringides, *Phys. Rev. B* **64**, 155307 (2001).
- [5] J. Kim, S. Qin, W. Yao, Q. Niu, M. Y. Chou, and C.-K. Shih, *Proc. Natl. Acad. Sci. USA* **107**, 12761 (2010).
- [6] M. H. Upton, C. M. Wei, M. Y. Chou, T. Miller, and T.-C. Chiang, *Phys. Rev. Lett.* **93**, 026802 (2004).
- [7] C. M. Wei and M. Y. Chou, *Phys. Rev. B* **66**, 233408 (2002).
- [8] Y. Jia, B. Wu, C. Li, T. L. Einstein, H. H. Weitering, and Z. Zhang, *Phys. Rev. Lett.* **105**, 066101 (2010).
- [9] L.-Y. Ma, L. Tang, Z.-L. Guan, K. He, K. An, X.-C. Ma, J.-F. Jia, Q.-K. Xue, Y. Han, S. Huang, and F. Liu, *Phys. Rev. Lett.* **97**, 266102 (2006).
- [10] P. Jiang, X. Ma, Y. Ning, C. Song, X. Chen, J.-F. Jia, and Q.-K. Xue, *J. Am. Chem. Soc.* **130**, 7790 (2008); X. Ma, P. Jiang, Y. Qi, J. Jia, Y. Yang, W. Duan, W.-X. Li, X. Bao, S. B. Zhang, and Q.-K. Xue, *Proc. Natl. Acad. Sci. USA* **104**, 9204 (2007).

- [11] A. A. Khajetoorians, W. Zhu, J. Kim, S. Qin, H. Eisele, Z. Zhang, and C.-K. Shih, *Phys. Rev. B* **80**, 245426 (2009).
- [12] P. S. Kirchmann, M. Wolf, J. H. Dil, K. Horn, and U. Bovensiepen, *Phys. Rev. B* **76**, 075406 (2007).
- [13] G. Kresse and J. Hafner, *Phys. Rev. B* **47**, 558 (1993).
- [14] G. Kresse and J. Furthmüller, *Phys. Rev. B* **54**, 11169 (1996); *Comput. Mater. Sci.* **6**, 15 (1996).
- [15] J. P. Perdew, in *Electronic Structure of Solids '91*, edited by P. Ziesche and H. Eschring (Akademie Verlag, Berlin, 1991).
- [16] G. Makov and M. C. Payne, *Phys. Rev. B* **51**, 4014 (1995).
- [17] D. Vanderbilt, *Phys. Rev. B* **41**, 7892 (1990).
- [18] T.-L. Chan, Y. X. Yao, C. Z. Wang, W. C. Lu, J. Li, X. F. Qian, S. Yip, and K. M. Ho, *Phys. Rev. B* **76**, 205119 (2007).
- [19] X. F. Qian, J. Li, L. Qi, C. Z. Wang, T. L. Chan, Y. X. Yao, K. M. Ho, and S. Yip, *Phys. Rev. B* **78**, 245112 (2008).
- [20] Y. X. Yao, C. Z. Wang, and K. M. Ho, *Phys. Rev. B* **81**, 235119 (2010).